Band parameters and electronic structures of wurtzite ZnO and ZnO/MgZnO quantum wells

W. J. Fan,[a] J. B. Xia,[b] P. A. Agus, S. T. Tan, S. F. Yu, and X. W. Sun
School of Electrical and Electronic Engineering, Nanyang Technological University, Singapore 639798, Singapore

(Received 17 May 2005; accepted 11 November 2005; published online 3 January 2006)

The band structures of wurtzite ZnO are calculated by the empirical pseudopotential method (EPM). The eight parameters of the Zn and O atomic pseudopotential form factors are obtained with the formula of Schluter *et al.*[Phys. Rev. B **12**, 4200 (1975)]. The band parameters are extracted by using a $k\cdot p$ Hamiltonian to fit the EPM results. The calculated band-edge energies (E_g, E_A, E_B, and E_C) at the Γ point are in good agreement with the experimental results. Based on the band parameters obtained, valence subbands of wurtzite $ZnO/Mg_xZn_{1-x}O$ tensile-strained quantum wells with different well widths and Mg compositions are calculated by the six-band $k\cdot p$ method.
 [DOI: 10.1063/1.2150266]

I. INTRODUCTION

Recently, ZnO has received great attention due to its potential applications in ultraviolet lasing optoelectronic devices and its unique physical properties. Huang *et al.* have observed room-temperature ultraviolet lasing from arrays of ZnO nanorods grown on sapphire substrates using a simple vapor transport and condensation process.[1] Yu *et al.* have shown that textured ZnO film might have higher quantum efficiency than GaN.[2] Bagnall *et al.* have reported a large exciton binding energy (around 60 meV) in ZnO.[3] Further, a negative spin-orbit (SO) splitting energy has been reported in ZnO.[4] The $k\cdot p$ method and effective-mass theory are very successful in the study of bulk and quantum well (QW) semiconductors.[5–9] However, the effective-mass parameters of ZnO for the $k\cdot p$ method are scarce in the literature. This could be the reason why there are few reports on the band structure of ZnO QW calculated by using the $k\cdot p$ method. In this work, we report the calculation of the band structures of wurtzite ZnO and give the effective-mass parameters. Based on the band parameters obtained, the hole subbands of wurtzite $ZnO/Mg_xZn_{1-x}O$ tensile-strained quantum wells with different well widths and Mg compositions are calculated by using the six-band $k\cdot p$ method.

II. BAND STRUCTURE OF BULK WURTZITE ZNO

Compared with zinc-blende semiconductors, wurtzite semiconductors have more complicated band structures because of the lack of inversion symmetry. For wurtzite ZnO, the crystal-field and spin-orbit splitting effects lead to a three-edge structure near the top of the valence band known as the A, B, and C edges in the literature, where A is the top of the valence band. The ordering is $A(\Gamma_7)$-$B(\Gamma_9)$-$C(\Gamma_7)$ due to a negative spin-orbit splitting, whose energies are given by

$$E_A(\Gamma_7) - E_B(\Gamma_9) = -\frac{\Delta_{so}+\Delta_{cf}}{2} + \frac{\sqrt{(\Delta_{so}+\Delta_{cf})^2 - \frac{8}{3}\Delta_{so}\Delta_{cf}}}{2}, \tag{1}$$

$$E_A(\Gamma_7) - E_C(\Gamma_7) = \sqrt{(\Delta_{so}+\Delta_{cf})^2 - \tfrac{8}{3}\Delta_{so}\Delta_{cf}}. \tag{2}$$

For ZnO, the experiment gave $E_A - E_B = 0.0024$ eV and $E_C = 0.0404$ eV.[10] Solving the above two equations, we have the crystal-field splitting energy $\Delta_{cf} = 0.0391$ eV and spin-orbit splitting energy $\Delta_{so} = -0.0035$ eV.

We represent the form factor of atomic pseudopotential with a continuous function of the wave vector q by the formula of Schluter *et al.*[11]

$$V(q) = \frac{\nu_1(q^2 - \nu_2)}{\exp[\nu_3(q^2 - \nu_4)] + 1}, \tag{3}$$

where the unit of q is a.u. and the unit of $V(q)$ is Ry. There are four parameters $\nu_1 - \nu_4$ for the Zn atom and four parameters for the O atom. Comparing the calculated energy bands with previous theoretical results[12,13] and experimental results,[10,14] we obtained that the Zn atomic pseudopotential parameters $\nu_1 - \nu_4$ are 0.110 03, 1.792 08, 0.7708, and 4.253 70, respectively. The O atomic pseudopotential parameters $\nu_1 - \nu_4$ are 0.196 29, 4.909 51, 1.244 75, and 3.600 95, respectively. The lattice constants a and c of ZnO used in our calculation are 3.25 and 5.21 Å, respectively. We give the eight parameters of atomic pseudopotential form factors with the formula of Schluter *et al.* Bloom and Ortenburger only listed the values of form factors at each reciprocal-lattice points.[12] We found that the O has deeply negative well, and the Zn has largely positive potential. Using the form factors, the band structure can be calculated by the empirical pseudopotential model (EPM), which is described in our previous work.[15,16] The calculated valence-band structures near the Γ point with and without SO interaction are shown in Fig. 1. In the case of zero SO coupling, see Fig. 1(a), the valence bands split into Γ_6 and Γ_1 levels at the top, separated by the Δ_{cf}. The Γ_6 level is twofold degenerate with the basis functions

[a]Electronic mail: ewjfan@ntu.edu.sg
[b]Present address: Institute of Semiconductors, Chinese Academy of Sciences, P.O. Box 912, Beijing 10083, China.

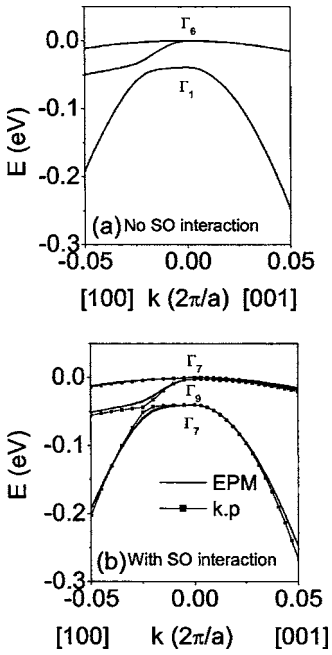

FIG. 1. The valence-band structures of wurtzite ZnO near the Γ point (a) without SO interaction (b) with SO interaction calculated by EPM (line) and fitted by the six-band $k\cdot p$ method (square+line).

of X and Y, and the Γ_1 level is single with the basis function of Z. We take the top of the valence band Γ_6 as the origin in our calculation. The calculated band gap $E_g=3.4421$ eV and $\Delta_{cf}=0.0391$ eV. The band-edge energies at the Γ points E_A, E_B, and E_C of wurtzite ZnO calculated by EPM are listed in Table I. Experimental results and other calculation results are also listed in the table for comparison. Our calculated electron effective masses perpendicular and along the c axis are $m_x^*=0.177m_0$ and $m_z^*=0.181m_0$, respectively, which are smaller than the electron mass of $0.24m_0$ in Ref. 18 and the experimental bare mass of $0.23m_0$ in Ref. 19. The reason caused by the smaller effective mass may be due to the ionic pseudopotential of the O ion. Figure 1(b) shows the band structures of wurtzite ZnO including SO interaction. The six-band Hamiltonian from Refs. 6,7,21 is used to fit the EPM results near the Γ point to extract effective-mass parameters. The six-band $k\cdot p$ fitting results are plotted with squares +lines, and the EPM calculation results are plotted with lines in Fig. 1(b). The effective-mass fitting parameters $A1$, $A2$, $A3$, $A4$, $A5$, and $A6$ are −6.680 36, −0.453 88, 6.127 50, −2.703 74, −2.766 90, and −4.625 66, respectively. The band

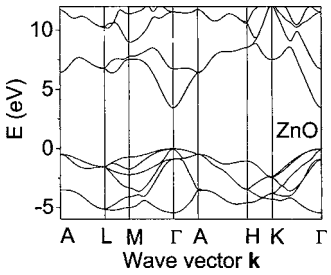

FIG. 2. Band structures of wurtzite ZnO including SO interaction.

structures of wurtzite ZnO including SO interaction are shown in Fig. 2.

III. BAND STRUCTURES OF WURTZITE ZNO/MG$_x$ZN$_{1-x}$O TENSILE-STRAINED QUANTUM WELLS

The in-plane valence-band dispersion curves of ZnO/$Mg_xZn_{1-x}O$-strained QW are calculated using the six-band $k\cdot p$ method including strain effect. The used ZnO parameters are listed in Table II. The in-plane lattice constant of $Mg_xZn_{1-x}O$, $a(Mg_xZn_{1-x}O)=3.250+0.036x$.[22] The band gap of $Mg_xZn_{1-x}O$, $E_g(Mg_xZn_{1-x}O)=3.34+2.00x$ (for hexagonal phase, $0\leqslant x\leqslant 0.33$), which is fitted from Ref. 25. In our calculation, we assume that the effective-mass parameters of the ZnO well region and MgZnO barrier region are the same. The band offset ratio is taken as 60:40 for conduction band over valence band. Assuming that the barrier material and substrate are the same, there is no strain in the barrier region. Because the lattice constant of ZnO is smaller than that of MgO, an in-plane tensile strain is formed in the ZnO well region only. Figure 3 shows the valence subband structures for ZnO/MgZnO QW with a well width of 40 Å, a barrier width of 200 Å, and the Mg mole fraction from (a) $x=0.1$, (b) $x=0.2$, and (c) $x=0.3$. The dispersions are plotted against the in-plane wave vector k_t. We take the hole energy positive. The identification of the subbands follows from the dominating composition of the wave function at the Γ point.[4] Unlike GaN/AlGaN compressive-strained QW, the first band ($n=1$) is LH*1* due to the negative Δ_{so} in ZnO. With increasing Mg composition x, the tensile strain in the QW increases which leads to reduce the light-hole energy and the heavy-hole energy. However, the Γ-point separation between the HH*i* and LH*i* subbands is not widened with x. This can be explained by the fact that the isotropic biaxial strain effects on HH and LH are the same: they cannot distinguish the

TABLE I. The band-edge energies at the Γ point, crystal field, and spin-orbit splitting energies for wurtzite ZnO.

	Present work without SO	Present work with SO	Experimental results	Other calculation results
E_g (eV)	3.4421	3.4409	3.44 (Ref. 10)	0.93(LDA) (Ref. 17), 4.23(GW) (Ref. 17), and 3.437 (Ref. 20)
E_A (eV)	0	0	0	0
E_B (eV)	0	−0.0023	−0.0024 (Ref. 10)	−0.013 (Ref. 18) and −0.010 (Ref. 20)
E_C (eV)	−0.0391	−0.0406	−0.0404 (Ref. 10)	−0.018 (Ref. 18) and −0.044 (Ref. 20)
Δ_{cf} (eV)	0.0391	0.0391	0.188 (Ref. 19)	0.027 (Ref. 18), 0.040 (Ref. 4), and 0.038 (Ref. 20)
Δ_{so} (eV)	0	−0.0035	−0.0035 (Ref. 19)	−0.019 (Ref. 18), −0.007 (Ref. 4), −0.009 15 (Ref. 20), and −0.013 59 (Ref. 20)

TABLE II. Material parameters for ZnO.

Parameters	ZnO
Lattice constant (Å) (Ref. 22)	
a	3.250
c	5.210
Energy parameters	
E_g(eV) at 300 K (Ref. 22,25)	3.34
Δ_1 ($=\Delta_{Cf}$) (meV) (this work)	39.10
Δ_{so}(meV) (Ref. 19)	−3.50
$\Delta_2=\Delta_3=\Delta_{so}/3$ (meV) (Ref. 19)	−1.17
Valence-band effective-mass parameters (this work)	
A_1	−6.680 36
A_2	−0.453 88
A_3	6.127 50
A_4	−2.703 74
A_5	−2.766 90
A_6	−4.625 66
Valence-band deformation potentials (eV) (Ref. 23)	
D_1	−2.66
D_2	2.82
D_3	−1.34
D_4	1.00
Elastic stiffness constants (GPa) (Ref. 24)	
C_{13}	105.1
C_{33}	210.9

energy levels. When increasing x the well potential will increase due to the larger band gap of MgO. The tensile strain in QW will enhance the increment. So, we observe more bound states in QW with increasing x.

Figure 4 shows the valence subbands of $ZnO/Mg_{0.2}Zn_{0.8}O$ QWs with the well widths L_W of (a) 40, (b) 60, and (c) 80 Å. The barrier width is fixed at 200 Å. The quantum size effect incorporated with the strained effect is clearly observed. When the well width is 80 Å, the valence subbands HHi or LHi) are very close together. With reducing the well width, the valence subbands start to move away from each other. However, we observed that a pair of LHi-HHi bands is formed with an almost fixed separation at the $k=0$ point, which can be understood using the above explanation of Fig. 3.

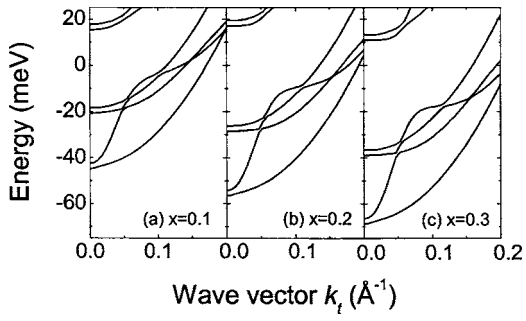

FIG. 3. The in-plane dispersion of valence subbands of $ZnO/Mg_xZn_{1-x}O$ QWs for (a) $x=0.1$, (b) $x=0.2$, and (c) $x=0.3$. The well width is fixed at 40 Å and the barrier width is fixed at 200 Å. From bottom to top, the subbands at the $k=0$ point are identified as LH1-HH1-LH2-HH2-LH3-HH3 for the three cases.

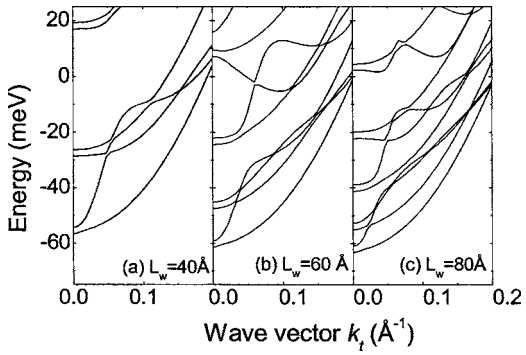

FIG. 4. The in-plane dispersion of valence subbands of $ZnO/Mg_{0.2}Zn_{0.8}O$ QW. The well width is varied from (a) 40, (b) 60, and (c) 80 Å. The barrier is fixed at 200 Å. From bottom to top, the subbands at $k=0$ point are identified as. (a) LH1-HH1-LH2-HH2-LH3-HH3, (b) LH1-HH1-LH2-HH2-LH3-HH3-LH4-HH4-CH1, and (c) LH1-HH1-LH2-HH2-LH3-HH3-LH4-HH4-LH5-CH1.

IV. CONCLUSIONS

The band structures of wurtzite ZnO are calculated by using the EPM. The parameters of the Zn and O atomic pseudopotential form factors are obtained. The calculated band gap is 3.4409 eV, the crystal-field splitting energy is 0.0391 eV, and the spin-orbit splitting energy is −0.0035 eV. These correspond to the band-edge energies $E_A=0$, $E_B=-0.0023$ ev, and $E_C=-0.004\,06$ eV. They are in good agreement with the experimental results. The A_1-A_6 effective-mass parameters are obtained. The hole subbands of wurzite $ZnO/Mg_xZn_{1-x}O$ tensile-strained quantum wells with different well widths and Mg compositions are calculated by using the six-band $k\cdot p$ method. A pair of LHi-HHi bands is formed with an almost fixed separation at the $k=0$ point, which can be explained by the fact that the isotropic biaxial strain effects on HH and LH energy levels are the same.

ACKNOWLEDGMENTS

One of the authors W.J.F. would like to thank Dr. Y. C. Yeo for the modifications of SO interaction program, another author J.B.X. would like to thank the National Natural Science Foundation of China No.90301007, and the special funds for Major State Basic Research Project of China No.G001CB3095.

[1] M. H. Huang *et al.*, Science **292**, 1897 (2001).
[2] P. Yu, Z. K. Tang, G. K. L. Wong, M. Kawaski, A. Ohtomo, and H. Koinuma, in *Physics of Semiconductors*, edited by M. Scheffer and R. Zimmermann (World Scientific, Singapore, 1996), p. 1453.
[3] D. M. Bagnall, Y. F. Chen, Z. Zhu, T. Yao, S. Koyama, M. Y. Shen, and T. Goto, Appl. Phys. Lett. **70**, 2230 (1997).
[4] L. C. L. Y. Yan, M. Willatzen, and M. Cardona, Phys. Rev. B **53**, 10703 (1996).
[5] S.-S. Li, B.-F. Zhu, and J.-B. Xia, J. Phys.: Condens. Matter **11**, 2809 (1999).
[6] Y. C. Yeo, T. C. Chong, M. F. Li, and W. J. Fan, J. Appl. Phys. **84**, 1813 (1998).
[7] Y. C. Yeo, T. C. Chong, M. F. Li, and W. J. Fan, IEEE J. Quantum Electron. **34**, 526 (1998).
[8] W. J. Fan, M. F. Li, T. C. Chong, and J. B. Xia, J. Appl. Phys. **80**, 3471 (1996).
[9] W. J. Fan and S. F. Yoon, J. Appl. Phys. **90**, 843 (2001).
[10] A. Mang, K. Reimann, and S. Rubenacke, Solid State Commun. **94**, 251 (1995).

[11]M. Schluter, J. R. Chelikowsky, S. G. Louie, and M. L. Cohen, Phys. Rev. B **12**, 4200 (1975).
[12]S. Bloom and I. Ortenburger, Phys. Status Solidi B **58**, 561 (1973).
[13]J. R. Chelikowsky, Solid State Commun. **22**, 351 (1977).
[14]K. Hummer, Phys. Status Solidi B **56**, 249 (1973).
[15]W. J. Fan, M. F. Li, T. C. Chong, and J. B. Xia, J. Appl. Phys. **79**, 188 (1996).
[16]J. R. Chelikowsky and M. L. Cohen, Phys. Rev. B **14**, 556 (1976).
[17]S. Massidda, R. Resta, M. Posternak, and A. Baldereschi, Phys. Rev. B **52**, R16977 (1995).
[18]U. Rossler, Phys. Rev. **184**, 733 (1969).
[19]Landolt-Bornstein, Group III, Vol. 22a, edited by K.-H. Hellwege (Springer-Verlag, Berlin, 1982).
[20]W. R. L. Lambrecht, A. V. Rodina, S. Limpijumnong, B. Segall, and B. K. Meyer, Phys. Rev. B **65**, 075207 (2002).
[21]J. B. Xia, K. W. Cheah, X. L. Wang, D. Z. Sun, and M. Y. Kong, Phys. Rev. B **59**, 10119 (1999).
[22]A. Ohomo and M. Kawaski, Appl. Phys. Lett. **75**, 890 (1999).
[23]J. E. Rowe, M. Cardona, and F. H. Pollak, Solid State Commun. **6**, 239 (1968).
[24]Landolt-Bornstein, Vol. 17 (Springer-Verlag, Berlin, 1982), p. 35.
[25]A. Ohtomo *et al.*, Appl. Phys. Lett. **72**, 2466 (1998).